JOURNAL OF GUIDANCE, CONTROL, AND DYNAMICS
Vol. 34, No. 2, March–April 2011

Optimal Cooperative Pursuit and Evasion Strategies Against a Homing Missile

Tal Shima*
Technion—Israel Institute of Technology, 32000 Haifa, Israel

DOI: 10.2514/1.51765

Optimal-control-based cooperative evasion and pursuit strategies are derived for an aircraft and its defending missile. The aircraft-defending missile team cooperates in actively protecting the aircraft from a homing missile. The cooperative strategies are derived assuming that the incoming homing missile is using a known linear guidance law. Linearized kinematics, arbitrary-order linear adversaries' dynamics, and perfect information are also assumed. Specific limiting cases are analyzed in which the attacking missile uses proportional navigation, augmented proportional navigation, or optimal guidance. The optimal one-on-one, noncooperative, aircraft evasion strategies from a missile using such guidance laws are also derived. For adversaries with first-order dynamics it is shown that depending on the initial conditions, and in contrast to the optimal one-on-one evasion strategy, the optimal cooperative target maneuver is either constant or arbitrary. These types of maneuvers are also the optimal ones for the defender missile. Simulation results confirm the usefulness and advantages of cooperation. Specifically, it is shown how the target can lure in the attacker, allowing its defender to intercept the attacking missile even in scenarios in which the defender's maneuverability is at a disadvantage compared with the attacking missile.

I. Introduction

AIRCRAFT protection from a homing interceptor is the topic of this paper. The aircraft may be a manned or unmanned aerial vehicle. To increase the aircraft's survivability it may employ electronic countermeasures, launch decoys, and perform evasive maneuvers. It may also launch a defending missile to intercept the incoming threat. These measures may be employed independently or cooperatively. In this paper we focus on deriving optimal cooperative strategies for an evading aircraft and a defending missile launched from the aircraft to intercept the incoming threat. It is expected that cooperation will improve the aircraft's probability of survival.

Guidance laws for intercepting a moving target, such as the defended aircraft in this study, have traditionally been developed for one-on-one engagements. Usually, optimal control theory is applied, and perfect information and linearized kinematics are assumed [1]. For example, the classical proportional navigation (PN) guidance law [2] is the optimal guidance law for a scenario between an interceptor with ideal dynamics and a nonmaneuvering target. The same is true for augmented proportional navigation (APN), if the target performs a constant maneuver [3]. Taking into account first-order interceptor dynamics, the well-known optimal guidance law (OGL) was obtained by Cottrell [4]. In [5] this work was extended to arbitrary known target maneuvers. All these guidance laws are linear and have the same general form of an effective navigation gain N' (constant or time-varying) multiplied by a zero-effort-miss term and divided by time-to-go squared.

Construction of the optimal evasive maneuver strategy, using optimal control theory, requires an assumption on the future behavior of the opponent. If the guidance law of the incoming homing interceptor is known to the aircraft, then it can perform the optimal evasion strategy. Such an analysis of a two-dimensional interception scenario in which the interceptor is assumed to use PN guidance was performed in [6–8]. In [6] the nonlinear engagement was studied numerically and different strategies were proposed for different engagement initial conditions. In [7] a model with linear kinematics and bounded pursuer (missile) and evader (aircraft) accelerations was analyzed. It was found analytically that the optimal evasion strategy has a bang–bang structure with a number of switches that is dependent on the value of N'. Closed-form solutions for the switching function and miss distance were obtained for the case of first-order missile dynamics and integer values of the effective navigation gain N'. In [8] the same model, but with nonlinear kinematics, was investigated. An equivalent linearized 3-D problem was analyzed in [9]. The optimal evasion strategy was identified as having a bang–bang structure in a plane, which, for a circular missile vectogram, is perpendicular to the initial plane of collision. The existence of an optimal maneuver plane renders the use of the results of the two-dimensional analysis applicable. Recently, the work of Shinar and Steinberg [7] on optimal evasion from a PN-guided missile was revisited [10,11]. The guaranteed miss distance was studied in the case in which the PN guidance system is subjected to bounded target maneuvers and bounded noise. And it was shown how a simple Simulink®-based block diagram of the minimal realization of the problem, with arbitrary-order missile dynamics, can be used to obtain the optimal evasion strategy and the guaranteed miss distance. Contrary to the relatively substantial work on optimal evasion from a PN-guided missile there is very little open literature on optimal evasion from other guidance laws. A noteworthy exception is [12], where optimal evasion in a nonlinear engagement between an aircraft and an APN-guided missile was studied numerically. The optimal evasion strategy was obtained by numerically solving the related nonlinear two-point boundary-value problem.

Asher and Matuszewski [5] discussed the use of a defender missile to protect a target aircraft from a homing missile. The closed-form kinematic relations in such an engagement with three entities (missile, target, and defender) moving in the plane, around a collision course, were studied in [13–15]. For the analysis it was assumed that the target is nonmaneuvering; no saturation limits exist for the missile and the defender; both the missile and the defender have ideal dynamics; and perfect information is available both to the missile about the target and to the defender about the missile. Conditions for the speed ratios were also derived for different attack geometries and a desired interception point. However, in realistic engagements the assumption of constant bearings is not valid, as vehicles are expected to maneuver in order to achieve their respective objectives.

In a series of papers, Rusnak [16–18] analyzed this problem using linear quadratic differential game (LQDG) theory. It was assumed

Received 26 July 2010; accepted for publication 18 October 2010.

*Senior Lecturer, Faculty of Aerospace Engineering; tal.shima@technion.ac.il. Associate Fellow AIAA.

that all three players (target, missile, and defender) can maneuver and the required acceleration level for each player was assessed. The guidance laws were established numerically by solving the relevant differential Riccati equation with impulse function utilization in the indices in order to reflect the defender's disappearance after its interception by the attacking missile. In a recent paper [19] an analytical solution to the LQDG problem was obtained. Arbitrary-order adversaries dynamics were considered and limiting cases were studied. Also, conditions for the existence of a saddle-point solution were derived and a nonlinear two-dimensional simulation was used to validate the theoretical analysis.

Line-of-sight (LOS) guidance is naturally suited to fit the target–missile–defender engagement, as by its very nature it is a three-point guidance strategy. In [20] the kinematics of LOS guidance with a moving/maneuvering launch platform was studied and the application of command to LOS guidance as a prospective defender guidance strategy in the target–missile–defender interception scenario was studied. Based on the kinematic results, a guidance law for the defended aircraft (the launch platform), cooperating with a LOS-guided defender in order to maximize the attacker-to-defender lateral acceleration ratio, was proposed and studied analytically and via simulation. In another recent work [21] the target–missile–defender interception problem was investigated for the case in which the target and its defender share noisy measurements on the attacking missile. The filter used was a nonlinear adaptation of a multiple-model adaptive estimator, in which each model represents a possible guidance law and guidance parameters of the incoming homing missile. A matched defender's missile guidance law was optimized to the identified homing missile guidance law. It uses cooperation between the aerial target and the defender stemming from the fact that the defender knows the future evasive maneuvers to be performed by the protected target. Thus, after identification was achieved (taking less than 2 s in the examined scenario), it can anticipate the maneuvers induced on the incoming homing missile. Moreover, the target performs a bang–bang maneuver with a single switch, with its timing chosen such that it minimizes the control effort required by the defender.

As the main contribution of this work we present the optimal cooperative evasion and pursuit strategies for the target and its defender missile, assuming that the attacking missile's guidance strategy is known. Linearized kinematics are assumed, as well as arbitrary-order linear adversaries' dynamics, and perfect information. As a special case, the optimal noncooperative one-on-one aircraft evasion strategy, from a missile employing a linear guidance strategy, such as APN or OGL, is also analytically derived, thus extending previous works [7,10] on optimal evasion from a PN-guided missile.

In the next section the target–missile–defender interception engagement is formulated. Next, in Sec. III, the analyzed linear missile guidance strategies are reviewed: specifically, PN, APN, and OGL. This is followed by the analytical derivation of optimal one-on-one, noncooperative, target evasion strategies from such missile guidance laws. Then, in Sec. V, the optimal cooperative target–defender evasion and pursuit strategies are derived and analyzed. Next, a simulation analysis is presented, followed by concluding remarks. In the appendices some special cases are analyzed.

II. Engagement Formulation

The problem consists of three entities: an evading target denoted as T, an attacking missile denoted as M, and a defending missile denoted as D. The attacking missile is chasing the target aircraft using a linear guidance strategy that is either known or has been identified. The target aircraft launches a defending missile to intercept the incoming threat. Obviously, the engagement between the defending missile and the attacking missile is planned to terminate before that between the attacking missile and the evading target.

We deal with the endgame of such a scenario and assume that the trajectories of the three entities can be linearized around the missile–target and defender–missile respective initial collision triangles. As the defending missile is fired from the evading aircraft, and for the sake of simplicity in order to avoid excessive notations, we assume that the missile–target initial LOS (ILOS) and defender–missile ILOS unite. We also assume perfect information and analyze the engagement in two dimensions.

In Fig. 1 a schematic view of the planar endgame geometry is shown, where the X axis is aligned with the ILOS used for linearization and Y is perpendicular to it. The notation MT denotes the attacking missile–evading target engagement, and MD denotes the attacking missile–defending missile engagement. The initial range between the missile and target is denoted as r_{MT}, and that between the defender missile and the attacking one is denoted as r_{MD}. We denote y_{MT} and y_{MD} as the target–missile and missile–defender relative displacement normal to the ILOS, respectively. The missile's, target's, and defender's accelerations perpendicular to the ILOS, are denoted as a_M, a_T, and a_D, respectively.

We assume that during the endgame the adversaries have constant speeds. Thus, after the respective collision triangles were reached and maintained, the missile–target closing speed (denoted $V_{C_{MT}}$) and that of the missile–defender ($V_{C_{MD}}$) are constant.

The missile–target interception time can be approximated by

$$t_{f_{MT}} = r_{MT}(0)/V_{C_{MT}} \tag{1}$$

and similarly

$$t_{f_{MD}} = r_{MD}(0)/V_{C_{MD}} \tag{2}$$

We define Δt as the time difference between interceptions

$$\Delta t = t_{f_{MT}} - t_{f_{MD}} \tag{3}$$

Note that $\Delta t > 0$, as we require the missile–target engagement to terminate after that of the missile–defender.

It is assumed that during the endgame the dynamics of each agent can be represented by arbitrary-order linear equations:

$$\dot{\boldsymbol{x}}_i = \mathbf{A}_i\boldsymbol{x}_i + \mathbf{B}_i u_i; \qquad i = \{M, T, D\} \tag{4}$$

$$a_i = \mathbf{C}_i\boldsymbol{x}_i + d_i u_i; \qquad i = \{M, T, D\} \tag{5}$$

where $\boldsymbol{x}_i$ is the state vector of an agent's internal state variables with $\dim(\boldsymbol{x}_i) = n_i$ and u_i is its controller. Note that in Eqs. (4) and (5), and in the remainder of this paper, bold is used to represent a vector/matrix.

The first term on the right-hand side of Eq. (5) is the part of the acceleration with dynamics, denoted as a_{iS}. We denote the second term on the right-hand side of Eq. (5) as the direct lift. This is the part of the acceleration without dynamics, i.e., the feedforward part. For example, in an aerodynamically controlled missile, and when neglecting servo dynamics, the direct lift is obtained immediately

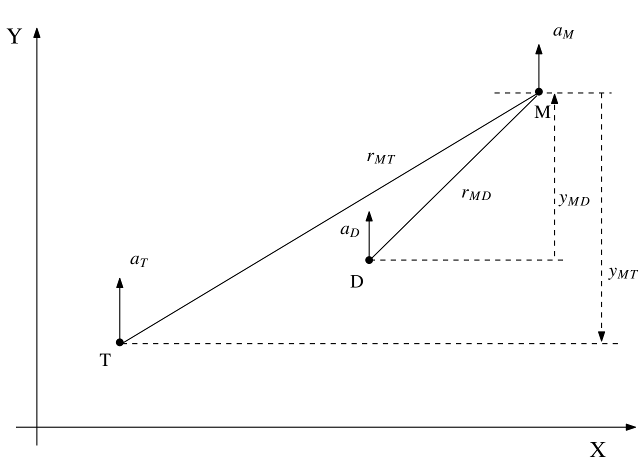

Fig. 1 Target–missile–defender engagement geometry.

from deflection of the canard or tail controls, and a_{iS} represents the response of the airframe.

The state vector of the target–missile–defender engagement is

$$\boldsymbol{x} = [y_{MT} \quad \dot{y}_{MT} \quad \boldsymbol{x}_M^T \quad \boldsymbol{x}_T^T \quad y_{MD} \quad \dot{y}_{MD} \quad \boldsymbol{x}_D^T]^T \tag{6}$$

Defining the state vector of the linearized missile–target engagement as

$$\boldsymbol{x}_{MT} = [y_{MT} \quad \dot{y}_{MT} \quad \boldsymbol{x}_M^T \quad \boldsymbol{x}_T^T]^T \tag{7}$$

and

$$\boldsymbol{x}_{MD} = [y_{MD} \quad \dot{y}_{MD} \quad \boldsymbol{x}_D^T]^T \tag{8}$$

we obtain

$$\boldsymbol{x} = [\boldsymbol{x}_{MT}^T \quad \boldsymbol{x}_{MD}^T]^T \tag{9}$$

The equations of motion (EOM) are

$$\dot{\boldsymbol{x}} = \begin{cases} \dot{x}_1 = x_2 \\ \dot{x}_2 = a_T - a_M \\ \dot{\boldsymbol{x}}_M = \mathbf{A}_M \boldsymbol{x}_M + \mathbf{B}_M u_M \\ \dot{\boldsymbol{x}}_T = \mathbf{A}_T \boldsymbol{x}_T + \mathbf{B}_T u_T \\ \dot{x}_{n_M+n_T+3} = x_{n_M+n_T+4} \\ \dot{x}_{n_M+n_T+4} = a_M - a_D \\ \dot{\boldsymbol{x}}_D = \mathbf{A}_D \boldsymbol{x}_D + \mathbf{B}_D u_D \end{cases} \tag{10}$$

These equations can be written in vector form as

$$\dot{\boldsymbol{x}} = \mathbf{A}\boldsymbol{x} + \mathbf{B}[u_T \quad u_D]^T + \mathbf{C}u_M \tag{11}$$

where

$$\mathbf{A} = \begin{bmatrix} \mathbf{A}_{MT} & [0] \\ \mathbf{A}_{21} & \mathbf{A}_{MD} \end{bmatrix}, \qquad \mathbf{B} = \begin{bmatrix} \mathbf{B}_{MT} & [0] \\ [0] & \mathbf{B}_{MD} \end{bmatrix}$$
$$\mathbf{C} = \begin{bmatrix} \mathbf{C}_{MT} \\ \mathbf{C}_{MD} \end{bmatrix} \tag{12}$$

and

$$\mathbf{A}_{MT} = \begin{bmatrix} 0 & 1 & [0] & [0] \\ 0 & 0 & -\mathbf{C}_M & \mathbf{C}_T \\ [0] & [0] & \mathbf{A_M} & [0] \\ [0] & [0] & [0] & \mathbf{A_T} \end{bmatrix}, \qquad \mathbf{B}_{MT} = \begin{bmatrix} 0 \\ d_T \\ [0] \\ \mathbf{B}_T \end{bmatrix}$$
$$\mathbf{C}_{MT} = \begin{bmatrix} 0 \\ -d_M \\ \mathbf{B}_M \\ [0] \end{bmatrix} \tag{13}$$

$$\mathbf{A}_{21} = \begin{bmatrix} [0] & [0] & [0] \\ [0] & \mathbf{C}_M & [0] \\ [0] & [0] & [0] \end{bmatrix}, \qquad \mathbf{A}_{MD} = \begin{bmatrix} 0 & 1 & [0] \\ 0 & 0 & -\mathbf{C}_D \\ [0] & [0] & \mathbf{A}_D \end{bmatrix}$$
$$\mathbf{B}_{MD} = \begin{bmatrix} 0 \\ -d_D \\ \mathbf{B}_D \end{bmatrix}, \qquad \mathbf{C}_{MD} = \begin{bmatrix} 0 \\ d_M \\ [0] \end{bmatrix} \tag{14}$$

with [0] denoting a matrix of zeros with appropriate dimensions.

III. Optimal Missile Guidance Law

Over the years many missile guidance laws have been developed. In this study we consider such linear guidance laws, commonly derived under the assumption of linear kinematics, perfect information, and unbounded controls [1]. Special attention is given to the most well-known guidance laws of PN [2], APN [3], and OGL [4].

These guidance laws have the following form [1]:

$$u_M = N_j' \frac{Z_j}{t_{go_{MT}}^2}; \qquad j = \{\text{PN, APN, OGL}\} \tag{15}$$

where N' is the effective navigation gain, $t_{go_{MT}}$ is the time-to-go defined in the missile–target engagement as

$$t_{go_{MT}} = t_{f_{MT}} - t \tag{16}$$

and Z is the well-known zero-effort-miss distance.

Remark 1. In such a one-sided linear optimization problem the zero-effort miss is the missile–target separation perpendicular to the ILOS at the final time $[y_{MT}(t_{f_{MT}})]$, which will be obtained if the attacking missile does not apply any control from the current time onward and the target aircraft continues employing the expected maneuver strategy that is known to the missile. The expression for the zero-effort miss is different for each guidance law, as it is dependent on the model used and assumptions made regarding the future target maneuvers.

Under the additional assumptions of ideal adversaries dynamics and no target maneuver (i.e., $u_T(t) = 0\ \forall t \geq 0$) the obtained optimal missile guidance law, guaranteeing zero miss distance and minimizing the control effort, is PN with

$$N'_{\text{PN}} = 3 \tag{17}$$

$$Z_{\text{PN}} = y_{MT} + \dot{y}_{MT} t_{go_{MT}} \tag{18}$$

Extending the results to the case in which the target is assumed to perform a constant maneuver, APN was obtained with

$$N'_{\text{APN}} = 3 \tag{19}$$

$$Z_{\text{APN}} = y_{MT} + \dot{y}_{MT} t_{go_{MT}} + a_T t_{go_{MT}}^2 / 2 \tag{20}$$

Further assuming that the missile's closed-loop acceleration dynamics can be approximated by a first-order proper transfer function with a time constant τ_M, OGL was obtained with

$$N'_{\text{OGL}} = \frac{6\theta_{MT}^2 \psi(\theta_{MT})}{3 + 6\theta_{MT} - 6\theta_{MT}^2 + 2\theta_{MT}^3 - 3e^{-2\theta_{MT}} - 12\theta_{MT} e^{-\theta_{MT}}} \tag{21}$$

$$Z_{\text{OGL}} = y_{MT} + \dot{y}_{MT} t_{go_{MT}} + a_T t_{go_{MT}}^2 / 2 - a_{MS} \tau_M^2 \psi(t_{go_{MT}} / \tau_M) \tag{22}$$

where θ_{MT} is the normalized time-to-go in the missile–target engagement:

$$\theta_{MT} = t_{go_{MT}} / \tau_M \tag{23}$$

and

$$\psi(\xi) = \exp(-\xi) + \xi - 1 \tag{24}$$

IV. Optimal Target Evasion Strategy

In this section we derive the optimal target evasion strategies from a missile employing a linear guidance law, such as those described in the previous section. The underlying assumption is that the missile's guidance strategy is known to the target, possibly using an online identification scheme. In [21], it was shown that in the target–missile–defender engagement the identification can be performed cooperatively by the target–defender team in less than 2 s.

A. Evasion Problem

The equations of motion in the missile–target engagement satisfy

$$\dot{\boldsymbol{x}}_{MT} = \mathbf{A}_{MT}\boldsymbol{x}_{MT} + \mathbf{B}_{MT}u_T + \mathbf{C}_{MT}u_M \tag{25}$$

We assume that the missile uses a linear guidance strategy of the form

$$u_M = \mathbf{K}(t_{\mathrm{go}_{MT}})\boldsymbol{x}_{MT} + K_{u_T}(t_{\mathrm{go}_{MT}})u_T \tag{26}$$

where

$$\mathbf{K}(t_{\mathrm{go}_{MT}}) = [K_1 \quad K_2 \quad \mathbf{K}_M \quad \mathbf{K}_T] \tag{27}$$

Remark 2. It is assumed here that the missile's current controller may be dependent on the target's current controller. Actually, if the missile uses an optimal-control-based guidance law (such as PN, APN, and OGL), then the underlying assumption in its derivation was that the target's controller is known not just at the current time but also from the current time until the end of the scenario.

Using Eq. (26) we obtain the EOM of the one-sided evasion problem:

$$\dot{\boldsymbol{x}}_{MT} = \mathbf{A}_E(t_{\mathrm{go}_{MT}})\boldsymbol{x}_{MT} + \mathbf{B}_E(t_{\mathrm{go}_{MT}})u_T \tag{28}$$

where

$$\mathbf{A}_E(t_{\mathrm{go}_{MT}}) = \begin{bmatrix} 0 & 1 & [0] & [0] \\ -d_M K_1 & -d_M K_2 & -\mathbf{C}_M - d_M\mathbf{K}_M & \mathbf{C}_T - d_M\mathbf{K}_T \\ \mathbf{B}_M K_1 & \mathbf{B}_M K_2 & \mathbf{A}_M + \mathbf{B}_M\mathbf{K}_M & \mathbf{B}_M\mathbf{K}_T \\ [0] & [0] & [0] & \mathbf{A_T} \end{bmatrix} \tag{29}$$

$$\mathbf{B}_E(t_{\mathrm{go}_{MT}}) = [0 \quad d_T - K_{u_T}d_M \quad K_{u_T}\mathbf{B}_M^T \quad \mathbf{B}_T^T]^T \tag{30}$$

We pose the optimal evasion problem as the maximization of the following cost function,

$$J = y_{MT}^2(t_{f_{MT}})/2 \tag{31}$$

subject to the EOM of Eq. (28) and under the constraint that the target's control u_T is bounded:

$$|u_T| \le u_T^{\max} \tag{32}$$

B. Reduced-Order Problem

We use the following transformation [22], sometimes denoted as *terminal projection*:

$$Z_{MT}(t) = \mathbf{D}_E\boldsymbol{\Phi}_E(t_{f_{MT}}, t)\boldsymbol{x}_{MT} \tag{33}$$

where $\mathbf{D}_E$ is a constant vector,

$$\mathbf{D}_E = [1 \quad 0 \quad [0]_{1\times n_M} \quad [0]_{1\times n_T}] \tag{34}$$

and $\boldsymbol{\Phi}_E(t_{f_{MT}}, t)$ is the transition matrix associated with Eq. (28),

$$\boldsymbol{\Phi}_E(t_{f_{MT}}, t) = \boldsymbol{\Phi}_E(t_{\mathrm{go}_{MT}}) = \begin{bmatrix} \phi_{11} & \phi_{12} & \boldsymbol{\phi}_{1M} & \boldsymbol{\phi}_{1T} \\ \phi_{21} & \phi_{22} & \boldsymbol{\phi}_{2M} & \boldsymbol{\phi}_{2T} \\ \boldsymbol{\phi}_{31} & \boldsymbol{\phi}_{32} & \boldsymbol{\phi}_{3M} & \boldsymbol{\phi}_{3T} \\ \boldsymbol{\phi}_{41} & \boldsymbol{\phi}_{42} & \boldsymbol{\phi}_{4M} & \boldsymbol{\phi}_{4T} \end{bmatrix} \tag{35}$$

satisfying

$$\dot{\boldsymbol{\Phi}}_E(t_{f_{MT}}, t) = -\boldsymbol{\Phi}_E(t_{f_{MT}}, t)\mathbf{A}_E(t_{go_{MT}}); \qquad \boldsymbol{\Phi}_E(t_{f_{MT}}, t_{f_{MT}}) = \mathbf{I} \tag{36}$$

Differentiating with respect to time the new zero-effort-miss state variable $Z_{MT}(t)$ of Eq. (33), and using Eq. (36), we obtain

$$\dot{Z}_{MT} = s_{MT}u_T \tag{37}$$

where

$$s_{MT} = \mathbf{D}_E\boldsymbol{\Phi}_E(t_{f_{MT}}, t)\mathbf{B}_E = (d_T - K_{U_T}d_M)\phi_{12} + K_{u_T}\boldsymbol{\phi}_{1M}\mathbf{B}_M + \boldsymbol{\phi}_{1T}\mathbf{B}_T \tag{38}$$

As expected, the dynamics of Eq. (37) are state-independent, as Z_{MT} is the homogeneous solution of Eq. (28).

As $Z_{MT}(t_{f_{MT}}) = y_{MT}(t_{f_{MT}})$ an equivalent reduced-order problem of finding the optimal target evasion strategy is the maximization of

$$J = Z_{MT}^2(t_{f_{MT}})/2 \tag{39}$$

subject to the scalar dynamics of Eq. (37) and the constraint of Eq. (32).

C. Solution

The Hamiltonian of the problem is

$$H = \lambda_{Z_{MT}}s_{MT}u_T \tag{40}$$

The adjoint equation and the transversality condition are

$$\dot{\lambda}_{Z_{MT}} = -\frac{\partial H}{\partial Z_{MT}} = 0; \qquad \lambda_{Z_{MT}}(t_{f_{MT}}) = Z_{MT}(t_{f_{MT}}) \tag{41}$$

yielding

$$\lambda_{Z_{MT}}(t) = Z_{MT}(t_{f_{MT}}) \tag{42}$$

The optimal target evasion strategy maximizes the Hamiltonian and thus satisfies

$$u_T^* = \arg_{u_T}\max H = u_T^{\max}\,\mathrm{sign}(s_{MT})\mathrm{sign}(Z_{MT}(t_{f_{MT}})) \tag{43}$$

where s_{MT} of Eq. (38) is the switching function.

The zero-effort-miss dynamics in *reverse time* satisfy

$$\frac{\mathrm{d}Z_{MT}}{\mathrm{d}t_{\mathrm{go}_{MT}}} = \frac{\mathrm{d}Z_{MT}}{\mathrm{d}t}\frac{\mathrm{d}t}{\mathrm{d}t_{\mathrm{go}_{MT}}} = -s_{MT}u_T \tag{44}$$

Integrating Eq. (44) with u_T^* of Eq. (43) until optimal trajectories intersect each other on the $Z_{MT} = 0$ axis, we obtain

$$\mathrm{sign}(Z_{MT}(t)) = \mathrm{sign}(Z_{MT}(t_{f_{MT}})) \quad \forall\ t \in [0, t_{f_{MT}}]; \quad Z_{MT}(0) \neq 0 \tag{45}$$

resulting in the closed-loop optimal evasion strategy:

$$u_T^* = u_T^{\max}\,\mathrm{sign}(s_{MT})\mathrm{sign}(Z_{MT}(t)); \qquad Z_{MT}(0) \neq 0 \tag{46}$$

Note that for $Z_{MT}(t) = 0$ the optimal target evasion strategy can be chosen as either $u_T^{\max}$ or $-u_T^{\max}$.

Remark 3. The optimal target evasion strategy of Eq. (46) was derived under the assumption of unbounded missile control command u_M. It was shown in [7] that if the missile acceleration a_M or its command u_M are bounded, then in order to exploit the missile's saturation the target maneuver switches should occur earlier in the engagement.

To implement the optimal evasion strategy we need to compute s_{MT} and Z_{MT}, using the ϕ_{12}, $\boldsymbol{\phi}_{1M}$, and $\boldsymbol{\phi}_{1T}$ elements of the transition matrix $\boldsymbol{\Phi}_E$. From Eq. (36) we obtain

$$\mathbf{D}_E \frac{\mathrm{d}\boldsymbol{\Phi}_E}{\mathrm{d}t_{\mathrm{go}_{MT}}} = \mathbf{D}_E \frac{\mathrm{d}\boldsymbol{\Phi}_E}{\mathrm{d}t} \frac{\mathrm{d}t}{\mathrm{d}t_{\mathrm{go}_{MT}}} = \mathbf{D}_E \boldsymbol{\Phi}_E(t_{f_{MT}}, t) \mathbf{A}_E(t_{\mathrm{go}_{MT}})$$
$$\boldsymbol{\Phi}_E(0) = \mathbf{I} \tag{47}$$

Consequently, we need to solve the following set of equations in reverse time:

$$\begin{cases} \frac{\mathrm{d}\phi_{11}}{\mathrm{d}t_{\mathrm{go}_{MT}}} = -d_M K_1 \phi_{12} + K_1 \boldsymbol{\phi}_{1M} \mathbf{B}_M; & \phi_{11}(0) = 1 \\ \frac{\mathrm{d}\phi_{12}}{\mathrm{d}t_{\mathrm{go}_{MT}}} = \phi_{11} - d_M K_2 \phi_{12} + K_2 \boldsymbol{\phi}_{1M} \mathbf{B}_M; & \phi_{12}(0) = 0 \\ \frac{\mathrm{d}\boldsymbol{\phi}_{1M}}{\mathrm{d}t_{\mathrm{go}_{MT}}} = [-\mathbf{C}_M - d_M \mathbf{K}_M]\phi_{12} + \boldsymbol{\phi}_{1M}[\mathbf{A}_M + \mathbf{B}_M \mathbf{K}_M]; & \boldsymbol{\phi}_{1M}(0) = [0] \\ \frac{\mathrm{d}\boldsymbol{\phi}_{1T}}{\mathrm{d}t_{\mathrm{go}_{MT}}} = [\mathbf{C}_T - d_M \mathbf{K}_T]\phi_{12} + \boldsymbol{\phi}_{1M} \mathbf{B}_M \mathbf{K}_T + \boldsymbol{\phi}_{1T} \mathbf{A}_T; & \boldsymbol{\phi}_{1T}(0) = [0] \end{cases} \tag{48}$$

where K_1, K_2, $\mathbf{K}_M$, and $\mathbf{K}_T$ of Eq. (27) are known functions of $t_{\mathrm{go}_{MT}}$ [given in Eq. (16)].

Using the optimal evasion strategy u_T^*, the optimal missile–target zero-effort-miss dynamics can be computed, satisfying

$$\dot{Z}^*_{MT} = \Gamma_{MT} \operatorname{sign}(Z_{MT}(t)) \tag{49}$$

where

$$\Gamma_{MT} = |s_{MT}| u_T^{\max} \tag{50}$$

Consequently, $|Z_{MT}|$ is a monotonically increasing function of time.

Defining

$$m = \int_0^{t_{f_{MT}}} \Gamma_{MT} \, \mathrm{d}t \tag{51}$$

we obtain the maximum miss distance as

$$\mathrm{Miss}_{MT} = |y_{MT}(t_{f_{MT}})| = |Z_{MT}(t_{f_{MT}})| = |Z_{MT}(0)| + m \tag{52}$$

Specific optimal evasion strategies against the linear guidance strategies discussed in the previous section: namely, PN, APN, and OGL, are provided in Appendix A.

V. Cooperative Optimal Pursuit and Evasion

We now turn our attention to deriving the optimal cooperative defender's pursuit strategy and the target's evasion strategy from a missile employing a linear guidance law, such as PN, APN, and OGL described in Section III. As in the previous section, the underlying assumption is that the missile's guidance strategy is known to the target–defender team, possibly using an online identification scheme [21].

A. Pursuit–Evasion Problem

The EOM of the missile–target–defender engagement are given in Eq. (11). We now assume that the missile uses a known linear guidance strategy of the form given in Eq. (26). Substituting Eq. (26) in Eq. (11) we obtain the EOM of the one-sided pursuit–evasion problem (from the point of view of the target–defender team)

$$\dot{\boldsymbol{x}} = \mathbf{A}_{\mathrm{PE}}(t_{\mathrm{go}})\boldsymbol{x} + \mathbf{B}_{\mathrm{PE}}(t_{\mathrm{go}})[\, u_T \quad u_D \,]^T \tag{53}$$

where

$$\mathbf{A}_{\mathrm{PE}}(t_{\mathrm{go}}) = \begin{bmatrix} \mathbf{A}_E(t_{\mathrm{go}} + \Delta t) & [0] \\ \mathbf{A}_{21} & \mathbf{A}_{MD} \end{bmatrix}$$
$$\mathbf{B}_{\mathrm{PE}}(t_{\mathrm{go}}) = \begin{bmatrix} \mathbf{B}_E(t_{\mathrm{go}} + \Delta t) & [0] \\ [0] & \mathbf{B}_{MD} \end{bmatrix} \tag{54}$$

t_{go} is the time-to-go in the defender–missile engagement defined as

$$t_{\mathrm{go}} = t_{f_{MD}} - t = t_{\mathrm{go}_{MT}} - \Delta t \tag{55}$$

$\mathbf{A}_{21}$, $\mathbf{A}_{MD}$, and $\mathbf{B}_{MD}$ are given in Eq. (14), and $\mathbf{A}_E$ and $\mathbf{B}_E$ are given in Eqs. (29) and (30), respectively.

We pose the optimal cooperative pursuit–evasion problem as the minimization of the following cost function,

$$J = y_{MD}^2(t_{f_{MD}})/2 \tag{56}$$

subject to the EOM of Eq. (53) and under the constraint that both the target's and defender's controls (u_T and u_D) are bounded:

$$|u_i| \leq u_i^{\max}; \qquad i = T, D \tag{57}$$

Remark 4. In minimizing J of Eq. (56) the defender (employing u_D and knowing the missile guidance strategy) is performing its classical role as a pursuer of the missile. In comparison, the target (employing u_T) to *minimize* the defender–missile separation (J of Eq. (56)) is using its knowledge on the missile guidance law to lure the missile to the vicinity of the defender. This is in contrast to the one-on-one engagement, where the target wishes to *maximize* the distance between the missile and itself.

B. Reduced-Order Problem

Using the *terminal projection* transformation we define the missile–defender zero-effort miss (Z_{MD}) as

$$Z_{MD}(t) = \mathbf{D}_{\mathrm{PE}} \boldsymbol{\Phi}_{\mathrm{PE}}(t_{f_{MD}}, t)\boldsymbol{x} \tag{58}$$

where

$$\mathbf{D}_{\mathrm{PE}} = [\, 0 \quad 0 \quad [0]_{1\times n_M} \quad [0]_{1\times n_T} \quad 1 \quad 0 \quad [0]_{1\times n_D} \,] \tag{59}$$

and $\boldsymbol{\Phi}_{\mathrm{PE}}(t_{f_{MD}}, t)$ is the transition matrix associated with Eq. (53):

$$\boldsymbol{\Phi}_{\mathrm{PE}}(t_{f_{MD}}, t) = \boldsymbol{\Phi}_{\mathrm{PE}}(t_{\mathrm{go}})$$
$$= \begin{bmatrix} \phi_{11} & \phi_{12} & \boldsymbol{\phi}_{1M} & \boldsymbol{\phi}_{1T} & \phi_{15} & \phi_{16} & \boldsymbol{\phi}_{1D} \\ \phi_{21} & \phi_{22} & \boldsymbol{\phi}_{2M} & \boldsymbol{\phi}_{2T} & \phi_{25} & \phi_{26} & \boldsymbol{\phi}_{2D} \\ \boldsymbol{\phi}_{31} & \boldsymbol{\phi}_{32} & \boldsymbol{\phi}_{3M} & \boldsymbol{\phi}_{3T} & \boldsymbol{\phi}_{35} & \boldsymbol{\phi}_{36} & \boldsymbol{\phi}_{3D} \\ \boldsymbol{\phi}_{41} & \boldsymbol{\phi}_{42} & \boldsymbol{\phi}_{4M} & \boldsymbol{\phi}_{4T} & \boldsymbol{\phi}_{45} & \boldsymbol{\phi}_{46} & \boldsymbol{\phi}_{4D} \\ \phi_{51} & \phi_{52} & \boldsymbol{\phi}_{5M} & \boldsymbol{\phi}_{5T} & \phi_{55} & \phi_{56} & \boldsymbol{\phi}_{5D} \\ \phi_{61} & \phi_{62} & \boldsymbol{\phi}_{6M} & \boldsymbol{\phi}_{6T} & \phi_{65} & \phi_{66} & \boldsymbol{\phi}_{6D} \\ \boldsymbol{\phi}_{71} & \boldsymbol{\phi}_{72} & \boldsymbol{\phi}_{7M} & \boldsymbol{\phi}_{7T} & \boldsymbol{\phi}_{75} & \boldsymbol{\phi}_{76} & \boldsymbol{\phi}_{7D} \end{bmatrix} \tag{60}$$

satisfying

$$\dot{\boldsymbol{\Phi}}_{\mathrm{PE}}(t_{f_{MD}}, t) = -\boldsymbol{\Phi}_{\mathrm{PE}}(t_{f_{MD}}, t)\mathbf{A}_{\mathrm{PE}}(t_{\mathrm{go}}); \qquad \boldsymbol{\Phi}_{\mathrm{PE}}(t_{f_{MD}}, t_{f_{MD}}) = \mathbf{I} \tag{61}$$

Differentiating with respect to time the missile–defender zero-effort-miss state variable ($Z_{MD}(t)$) of Eq. (58), and using Eq. (61), we obtain

$$\dot{Z}_{MD} = \mathbf{S}_{MD}[\, u_T \quad u_D \,]^T \tag{62}$$

where

$$\mathbf{S}_{MD} = \mathbf{D}_{\mathrm{PE}} \boldsymbol{\Phi}_{\mathrm{PE}}(t_{f_{MD}}, t)\mathbf{B}_{\mathrm{PE}} = [\, s_{MD_1} \quad s_{MD_2} \,] \tag{63}$$

and

$$s_{MD_1} = (d_T - K_{U_T} d_M)\phi_{52} + K_{u_T} \boldsymbol{\phi}_{5M} \mathbf{B}_M + \boldsymbol{\phi}_{5T} \mathbf{B}_T \tag{64}$$

$$s_{MD_2} = -\phi_{56} d_D + \boldsymbol{\phi}_{5D} \mathbf{B}_D \tag{65}$$

As $Z_{MD}(t_{f_{MD}}) = y_{MD}(t_{f_{MD}})$ an equivalent reduced-order problem of finding the optimal cooperative defender's pursuit strategy and the target's evasion strategy, is the minimization of

$$J = Z_{MD}^2(t_{f_{MD}})/2 \tag{66}$$

subject to the scalar dynamics of Eq. (62) and the constraints of Eq. (57).

C. Solution

The Hamiltonian of the problem is

$$H = \lambda_{Z_{MD}}(s_{MD_1}u_T + s_{MD_2}u_D) \tag{67}$$

The adjoint equation and the transversality condition are

$$\dot{\lambda}_{Z_{MD}} = -\frac{\partial H}{\partial Z_{MD}} = 0; \qquad \lambda_{Z_{MD}}(t_{f_{MD}}) = Z_{MD}(t_{f_{MD}}) \tag{68}$$

yielding

$$\lambda_{Z_{MD}}(t) = Z_{MD}(t_{f_{MD}}) \tag{69}$$

The optimal target and defender strategies minimize the Hamiltonian and thus satisfy

$$u_T^* = \arg_{u_T} \min H = -u_T^{\max} \operatorname{sign}(s_{MD_1})\operatorname{sign}(Z_{MD}(t_{f_{MD}})) \tag{70}$$

$$u_D^* = \arg_{u_D} \min H = -u_D^{\max} \operatorname{sign}(s_{MD_2})\operatorname{sign}(Z_{MD}(t_{f_{MD}})) \tag{71}$$

where s_{MD_1} and s_{MD_2} are the switching functions of the target and defender, defined in Eqs. (64) and (65), respectively.

Using the optimal strategies u_T^* and u_D^* the optimal missile–defender zero-effort-miss dynamics can be computed in *reverse time*, satisfying

$$\begin{aligned} &\frac{\mathrm{d}Z_{MD}^*}{\mathrm{d}t_{\mathrm{go}}} = \frac{\mathrm{d}Z_{MD}^*}{\mathrm{d}t}\frac{\mathrm{d}t}{\mathrm{d}t_{\mathrm{go}}} = \Gamma_{MD}\operatorname{sign}(Z_{MD}(t_{\mathrm{go}}=0)); \\ &Z_{MD}(t_{\mathrm{go}}=0) \neq 0 \end{aligned} \tag{72}$$

where

$$\Gamma_{MD} = \Gamma_{MD1} + \Gamma_{MD2} \tag{73}$$

and

$$\Gamma_{MD1} = |s_{MD_1}|u_T^{\max} \tag{74}$$

$$\Gamma_{MD2} = |s_{MD_2}|u_D^{\max} \tag{75}$$

Note that contrary to $|Z_{MT}|$ of the previous section, here $|Z_{MD}|$ is a monotonically increasing function of time-to-go (decreasing function of time).

We now define the optimal border trajectory:

$$Z_{MD}^*(t_{\mathrm{go}}) = \int_0^{t_{\mathrm{go}}} \Gamma_{MD}\,\mathrm{d}t_{\mathrm{go}} = \int_0^{t_{\mathrm{go}}} \Gamma_{MD1}\,\mathrm{d}t_{\mathrm{go}} + \int_0^{t_{\mathrm{go}}} \Gamma_{MD2}\,\mathrm{d}t_{\mathrm{go}} \tag{76}$$

In the region defined by $|Z_{MD}(t_{\mathrm{go}})| > Z_{MD}^*(t_{\mathrm{go}})$ we obtain, when using the optimal strategies of Eqs. (70) and (71), that $\operatorname{sign}(Z_{MD}(t)) = \operatorname{sign}(Z_{MD}(t_{f_{MD}}))$. In the region between the two border trajectories Z_{MD}^* and $-Z_{MD}^*$ (i.e., $|Z_{MD}(t_{\mathrm{go}})| < Z_{MD}^*(t_{\mathrm{go}})$) every target and defender strategy will lead, eventually, to the border trajectories Z_{MD}^* or $-Z_{MD}^*$ and the target and defender can use arbitrary strategies. We denote this region as being singular.

Consequently, the optimal closed-loop strategies satisfy

$$u_T^* = \begin{cases} -u_T^{\max}\operatorname{sign}(s_{MD_1})\operatorname{sign}(Z_{MD}(t)) & |Z_{MD}(t_{\mathrm{go}})| \geq Z_{MD}^*(t_{\mathrm{go}}) \\ \text{arbitrary} & |Z_{MD}(t_{\mathrm{go}})| < Z_{MD}^*(t_{\mathrm{go}}) \end{cases} \tag{77}$$

$$u_D^* = \begin{cases} -u_D^{\max}\operatorname{sign}(s_{MD_2})\operatorname{sign}(Z_{MD}(t)) & |Z_{MD}(t_{\mathrm{go}})| \geq Z_{MD}^*(t_{\mathrm{go}}) \\ \text{arbitrary} & |Z_{MD}(t_{\mathrm{go}})| < Z_{MD}^*(t_{\mathrm{go}}) \end{cases} \tag{78}$$

Remark 5. If the engagement is initialized in the singular region, then the missile–defender miss distance will be null and the target can issue, until one of the border trajectories is reached, its optimal one-on-one optimal evasion strategy, given in Eq. (46).

Using the above optimal strategies, the optimal minimum miss distance between the defender and the missile is

$$\begin{aligned} \mathrm{Miss}_{MD} &= |y_{MD}(t_{f_{MD}})| \\ &= \begin{cases} |Z_{MD}(t=0)| - Z_{MD}^*(t=0) & |Z_{MD}(t=0)| > Z_{MD}^*(t=0) \\ 0 & |Z_{MD}(t=0)| \leq Z_{MD}^*(t=0) \end{cases} \end{aligned} \tag{79}$$

To implement the optimal target and defender strategies we need to compute the ϕ_{52}, $\boldsymbol{\phi}_{5M}$, $\boldsymbol{\phi}_{5T}$, ϕ_{56}, and $\boldsymbol{\phi}_{5D}$ elements of the transition matrix $\boldsymbol{\Phi}_{\mathrm{PE}}$. Using Eq. (61) we obtain

$$\begin{aligned} \mathbf{D}_{\mathrm{PE}}\frac{\mathrm{d}\boldsymbol{\Phi}_{\mathrm{PE}}}{\mathrm{d}t_{\mathrm{go}}} = \mathbf{D}_{\mathrm{PE}}\frac{\mathrm{d}\boldsymbol{\Phi}_{\mathrm{PE}}}{\mathrm{d}t}\frac{\mathrm{d}t}{\mathrm{d}t_{\mathrm{go}}} &= \mathbf{D}_{\mathrm{PE}}\boldsymbol{\Phi}_{\mathrm{PE}}(t_{f_{MD}}, t)\mathbf{A}_{\mathrm{PE}}(t_{\mathrm{go}}) \\ \boldsymbol{\Phi}_{\mathrm{PE}}(0) &= \mathbf{I} \end{aligned} \tag{80}$$

Consequently,

$$\begin{cases} \frac{\mathrm{d}\phi_{51}}{\mathrm{d}t_{\mathrm{go}}} = -d_M K_1 \phi_{52} + K_1 \phi_{1M}\mathbf{B}_M \\ \frac{\mathrm{d}\phi_{52}}{\mathrm{d}t_{\mathrm{go}}} = \phi_{51} - d_M K_2 \phi_{52} + K_2 \boldsymbol{\phi}_{5M}\mathbf{B}_M \\ \frac{\mathrm{d}\boldsymbol{\phi}_{5M}}{\mathrm{d}t_{\mathrm{go}}} = [-\mathbf{C}_M - d_M\mathbf{K}_M]\phi_{52} + \boldsymbol{\phi}_{5M}[\mathbf{A}_M + \mathbf{B}_M\mathbf{K}_M] + \phi_{56}\mathbf{C}_M \\ \frac{\mathrm{d}\boldsymbol{\phi}_{5T}}{\mathrm{d}t_{\mathrm{go}}} = [\mathbf{C}_T - d_M\mathbf{K}_T]\phi_{52} + \boldsymbol{\phi}_{5M}\mathbf{B}_M\mathbf{K}_T + \boldsymbol{\phi}_{5T}\mathbf{A}_T \\ \frac{\mathrm{d}\phi_{55}}{\mathrm{d}t_{\mathrm{go}}} = 0 \\ \frac{\mathrm{d}\phi_{56}}{\mathrm{d}t_{\mathrm{go}}} = \phi_{55} \\ \frac{\mathrm{d}\boldsymbol{\phi}_{5D}}{\mathrm{d}t_{\mathrm{go}}} = -\phi_{56}\mathbf{C}_D + \boldsymbol{\phi}_{5D}\mathbf{A}_D \end{cases} \tag{81}$$

with all initial conditions being equal to zero, except for ϕ_{55}, where $\phi_{55}(0) = 1$. Note that K_1, K_2, $\mathbf{K}_M$, and $\mathbf{K}_T$ of Eq. (27) are known functions of $t_{\mathrm{go}_{MT}}$ (i.e., $t_{\mathrm{go}} + \Delta t$).

Obviously, the solutions for ϕ_{55} and ϕ_{56} are

$$\phi_{55} = 1 \tag{82}$$

$$\phi_{56} = t_{\mathrm{go}} \tag{83}$$

Remark 6. If the attacking missile is not intercepted by the defender by the end of the cooperative engagement ($t = t_{fMD}$), then in the remaining time Δt the target should employ the optimal one-on-one evasion strategy of Eq. (46). Actually, the target can anticipate from the beginning of the cooperative pursuit–evasion engagement if the defender is expected to intercept the missile. If not, then it can switch to its optimal one-on-one evasion strategy already from the beginning of the engagement.

D. Special Cases

If Eq. (A2) holds [i.e., $K_2 = K_1 \cdot (t_{\mathrm{go}} + \Delta t)$], as in the case of a missile guided by PN, APN, or OGL, then

$$\phi_{52} = \phi_{51} \cdot (t_{\mathrm{go}} + \Delta t) \tag{84}$$

and we are left with the following set of equations:

$$\begin{cases} \frac{d\phi_{52}}{dt_{go}} = [1/(t_{go} + \Delta t) - d_M K_2]\phi_{52} + K_2 \boldsymbol{\phi}_{5M} \mathbf{B}_M; & \phi_{52}(0) = 0 \\ \frac{d\boldsymbol{\phi}_{5M}}{dt_{go}} = [-\mathbf{C}_M - d_M \mathbf{K}_M]\phi_{52} + \boldsymbol{\phi}_{5M}[\mathbf{A}_M + \mathbf{B}_M \mathbf{K}_M] + t_{go}\mathbf{C}_M; & \boldsymbol{\phi}_{5M}(0) = [0] \\ \frac{d\boldsymbol{\phi}_{5T}}{dt_{go}} = [\mathbf{C}_T - d_M \mathbf{K}_T]\phi_{52} + \boldsymbol{\phi}_{5M}\mathbf{B}_M \mathbf{K}_T + \boldsymbol{\phi}_{5T}\mathbf{A}_T; & \boldsymbol{\phi}_{5T}(0) = [0] \\ \frac{d\boldsymbol{\phi}_{5D}}{dt_{go}} = -t_{go}\mathbf{C}_D + \boldsymbol{\phi}_{5D}\mathbf{A}_D; & \boldsymbol{\phi}_{5D}(0) = [0] \end{cases} \tag{85}$$

In such a case the missile–defender zero-effort-miss distance is

$$Z_{MD} = \phi_{52}[\dot{y}_{MT} + y_{MT}/(t_{go} + \Delta t)] + \phi_{5M}\boldsymbol{x}_M + \boldsymbol{\phi}_{5T}\boldsymbol{x}_T + y_{MD} + \dot{y}_{MD}t_{go} + \boldsymbol{\phi}_{5D}\boldsymbol{x}_D \tag{86}$$

Note that the first two equations in Eqs. (85) are independent from the rest, as well as the fourth one. For a defender missile with ideal dynamics $\boldsymbol{\phi}_{5D} = 0$ and for a defender with first-order strictly proper dynamics (i.e., $\mathbf{A}_D = -1/\tau_D$, $\mathbf{B}_D = 1/\tau_D$, $\mathbf{C}_D = 1$, $d_D = 0$), we obtain

$$\phi_{5D} = -\tau_D^2 \psi(t_{go}/\tau_D) \tag{87}$$

where ψ is given in Eq. (24). In such a case,

$$s_{MD2} = -\tau_D \psi(t_{go}/\tau_D) \tag{88}$$

and

$$\int_0^{t_{go}} \Gamma_{MD2}\, dt_{go} = u_D^{max}[t_{go}^2/2 - \tau_D^2 \psi(t_{go}/\tau_D)] \tag{89}$$

Note that since $\psi(\xi) > 0\ \forall\, \xi > 0$, then s_{MD_2} is a negative definite function. Therefore, until the zero-effort-miss distance is null, the defender will not change the direction of its maneuver command, which is dependent on the initial value of the zero-effort-miss. After Z_{MD} reaches zero the defender no longer issues maneuver commands.

The specific cooperative strategies for the cases in which the missile uses PN, APN, or OGL are provided in Appendix B.

VI. Simulation Analysis

In this section using simulation we analyze the optimal cooperative target and defender pursuit–evasion strategies and the optimal one-on-one target evasion strategy derived in the previous sections. We also illustrate the qualitative nature of optimal trajectories in the respective zero-effort miss vs time-to-go plane.

For the analysis we assume that the attacking missile, target aircraft, and defending missile have first-order acceleration dynamics. In the simulations we apply acceleration saturation. We assume that the acceleration command of the target is limited to 5 g (i.e., $u_T^{max} = 5\ g$), and the missile has five times the maneuver advantage (i.e., $u_M^{max} = 25\ g$). To show the benefit of cooperation and the ability to protect the target with a defender having a very limited maneuver capability we choose a 3 g acceleration command limit for the defender missile ($u_D^{max} = 3\ g$). In the cooperative engagement the time difference Δt between the engagements is a half-second. Note that all plots are in reverse time, i.e., time-to-go, where $t_{go} = 0$ represents the end of the cooperative engagement between the defender–target team and the missile.

As mentioned earlier, the underlying assumption in the derivation was that the missile's guidance strategy is known to the target, possibly using an online identification scheme. Thus, if identification is needed, then the simulated engagement takes place after identification has been achieved.

In the next subsection we first examine the one-on-one engagement between the target aircraft and the attacking missile. Then we demonstrate the capability of protecting such a target by a cooperating defender missile.

A. One-on-One Optimal Evasion

OGL was derived for the investigated case with a missile having a first-order strictly proper acceleration transfer function. Thus, it yields a zero miss distance against any target maneuver. Such a case necessitates the use of a defender missile. In this subsection we examine the one-on-one engagement. Thus, we investigate only optimal target evasion from a missile that is using either PN or APN guidance with an effective navigation gain N' of 4. General results and those of a sample run are provided next.

For the target to employ the optimal evasion strategy of Eq. (46) we need to compute the switching function s_{MT}, given in Eqs. (A9) and (A14) for PN and APN, respectively. We also need to compute the target–missile zero-effort miss Z_{MT}, which has an identical expression for PN and APN, given in Eq. (A10). To that end the ϕ_{12}, ϕ_{1M}, and ϕ_{1T} elements of the transition matrix $\boldsymbol{\Phi}_E$ need be computed. The time evolution of these elements is given in Fig. 2. Note that the plotted numerical solutions for ϕ_{12} and ϕ_{1M} are identical to the closed-form solutions of Eqs. (A5) and (A6), respectively.

Figure 3 presents results of sample runs for a comparison between optimal evasion from a missile employing PN vs APN guidance. The upper frame presents a comparison between the switching surfaces computed based on Eqs. (A9) and (A14). The difference between the surfaces is evident: the switching surface changes sign twice for PN three times for APN, and the optimal timings for the switches are different. Consequently, against PN the optimal target maneuver is composed of two sign changes, compared with three for APN, as is evident in the middle frame showing the time evolution of the target and missile accelerations. The time evolution of the zero-effort miss Z_{MT} for these engagements is given in the bottom frame. As expected, it is evident that $|Z_{MT}|$ increases monotonically. Note that for this example, optimal evasion from APN leads to a smaller miss distance (0.32 m) than when evading from a PN-guided missile (0.35 m). However, changing the value of the navigation gain can lead to an opposite result.

Optimal trajectories in the zero-effort miss vs time-to-go plane are plotted in Fig. 4 for different initial conditions. The top frame presents trajectories for PN, and the bottom one for APN. In each frame all trajectories are parallel to each other and lead to a nonzero miss distance. Note that the engagement will remain on such optimal trajectories as long as the target performs the optimal evasion strategy, using the switching function plotted in the top frame of Fig. 3, and the missile sticks to its known guidance strategy.

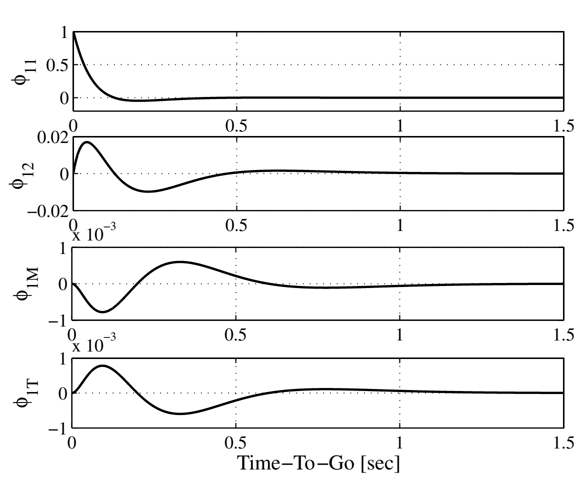

Fig. 2 Time evolution of evasion relevant transition matrix elements.

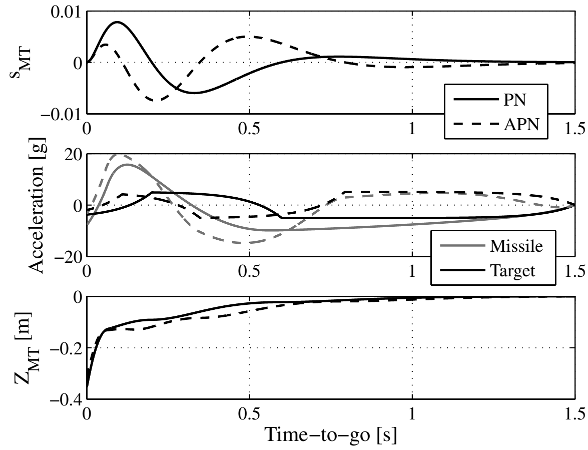

Fig. 3 Comparison between evasion from PN- and APN-guided missiles.

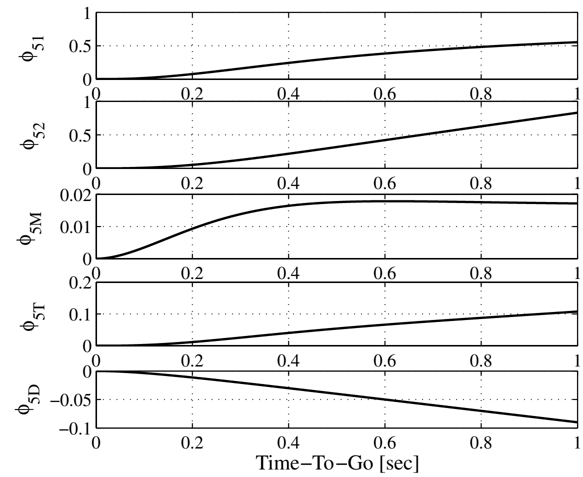

Fig. 5 Time evolution of pursuit–evasion relevant transition matrix elements.

B. Cooperative Optimal Pursuit and Evasion

We now examine the target–missile–defender engagement. It is assumed that the missile is using APN guidance with a navigation constant N' of 4, and the target aircraft and its defending missile are using the optimal strategies given in Eqs. (77) and (78), respectively. General results and those of a sample run are provided next.

The transition matrix elements that are relevant for performing the optimal pursuit and evasion strategies are plotted in Fig. 5. These elements are needed for the computation of the zero-effort miss between the defender and the missile (Z_{MD}) and the target and defender switching surfaces (s_{MD1} and s_{MD2}). Note that all elements do not change sign during the engagement. In particular, as ϕ_{5D} (plotted in the bottom frame) does not change sign, then the switching surface for the defender [given in Eq. (88)] does not change sign and the defender performs a constant maneuver, with its direction being dependent on the initial value of Z_{MD}.

The switching surfaces, acceleration profiles, and zero-effort-miss time evolutions are plotted in Fig. 6 for a sample run. In the top frame the target and defender switching surfaces [s_{MD1} from Eq. (B3) and s_{MD2} from Eq. (88), respectively], that are applicable for the cooperative case, are plotted. Also plotted in this frame is the switching surface s_{MT}, applicable for the target for the last half-second (as $\Delta t = 0.5$ s) from when the defender–target engagement terminates. From that point of time until the end of the scenario the target can perform the optimal one-on-one evasion strategy. To enable the plot in the same frame the value of s_{MT} is multiplied by 100. Note that the switching surfaces for the cooperative strategies do not change sign, yielding constant target and defender maneuvers, until the $Z_{MD} = 0$ axis is reached (see bottom frame). Once $Z_{MD} = 0$, the target and defender do not apply controls and their accelerations converge exponentially to zero, as can be seen from the middle frame. Once the defender–missile engagement terminates (i.e., $t_{go} = 0$) the target stops aiding the defender and starts performing an optimal bang–bang maneuver in the remaining time until interception by the missile. Note that due to the cooperation, the miss distance between the defender and missile is nulled ($Z_{MD} = 0$), and the miss distance between the target and the missile is 0.2 m [i.e., $Z_{MT}(t_{f_{MT}}) = 0.2$ m. This miss distance is smaller than for the case presented in the previous section, where the target performed the optimal one-on-one evasion strategy [$Z_{MT}(t_{f_{MT}}) = 0.32$ m] for the entire engagement duration. Note that for comparative reasons in the bottom frame the results of Z_{MT} are multiplied by 100.

Figure 7 presents the optimal trajectories, in the missile–defender zero-effort miss vs time-to-go plane, for different initial conditions. Optimal trajectories in this plane (that are parallel to each other) are plotted using a solid line, with the border trajectories Z^*_{MD} and $-Z^*_{MD}$ [given in Eq. (76)] highlighted using a thicker line. The time evolution of the zero-effort miss of the sample run is plotted using a dashed line. In the singular region between the border trajectories Z^*_{MD} and $-Z^*_{MD}$, any target and defender strategy is optimal, as eventually these border trajectories will be reached and maintained. Thus, all initial conditions in this region will lead to a zero miss distance in the defender–missile engagement. In such a case the target can instead apply its optimal one-on-one optimal evasion strategy, for example. Outside this singular region the target and defender must apply a unique strategy of a maximum maneuver command [see Eqs. (77) and (78), respectively]. It should be noted

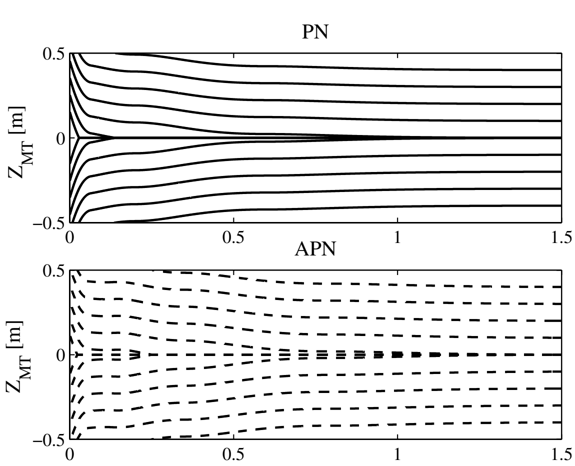

Fig. 4 Comparison between PN and APN optimal trajectories in the zero-effort miss vs time-to-go plane.

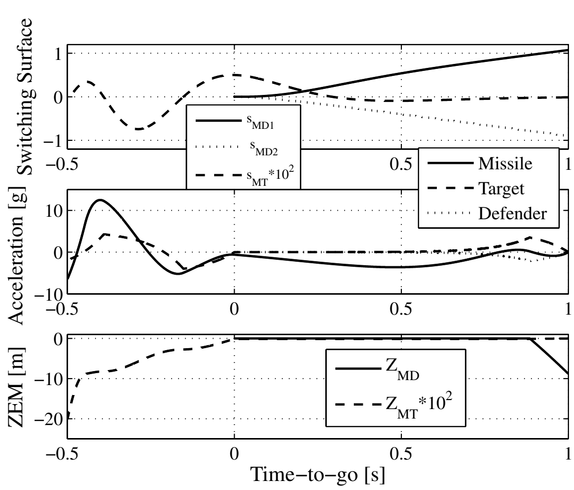

Fig. 6 Sample run of switching surface, acceleration, and zero-effort-miss profiles; cooperative engagement.

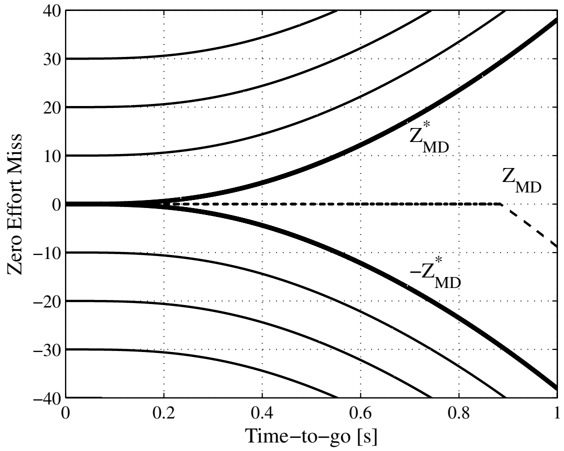

Fig. 7 Optimal trajectories in the missile–defender zero-effort miss vs time-to-go plane.

that qualitatively similar results have been obtained for the cases in which the missile uses either PN or OGL instead of APN and the target–defender team uses the respective optimal cooperative strategies.

C. Noncooperative Pursuit and Evasion

We would now like to compare the cooperative scenario with a noncooperative one. The results of a sample scenario with no cooperation between the target and the defender are plotted in Fig. 8. The initial conditions are the same as those in the engagement plotted in Fig. 6. In this noncooperative scenario the target performs the optimal one-on-one optimal evasion strategy, and the defender uses APN for guidance with an effective navigation gain of 4. It is evident from the middle frame that the target's evasive maneuvers induce harsher maneuvers from the missile, up to about 20 g, compared with about 12 g in the cooperative engagement (see middle frame of Fig. 6). Consequently, as can be seen from the bottom frame, the defender–missile miss distance is seriously affected. It is now 4.3 m ($Z_{MD}(t_{f_{MD}}) = 4.3$ m), compared with zero when the target and defender cooperated. Note that performing the optimal one-on-one optimal evasion strategy has only a small effect on the missile–target miss distance, raising it from 0.2 to 0.32 m.

For the same initial conditions similar qualitative results have been obtained for the cases in which instead of APN the missile is using either PN (with $N' = 4$) or OGL. In such cases, if the target issues the appropriate PN or OGL optimal evasive maneuver, then the missile–defender miss distance is 17.2 or 5.05 m, respectively. This is in comparison with a zero miss distance achieved if the target and defender cooperate. In all these cases the missile–target miss distance is near zero (it is identical to zero in the case of OGL), necessitating the use of a cooperating defender missile.

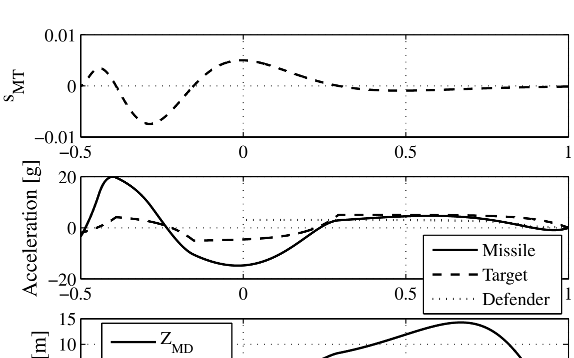

Fig. 8 Sample run of switching surface, acceleration, and zero-effort-miss profiles; noncooperative engagement.

VII. Conclusions

Optimal evasion and pursuit strategies for a target aircraft and its defender missile, cooperating in protecting the target from an incoming missile, have been derived. The problem was analyzed for arbitrary-order linear adversaries dynamics and assuming perfect information. The cooperative strategies are applicable when the missile is using a known linear strategy, such as proportional navigation, augmented proportional navigation, or optimal guidance law. The optimal one-on-one, noncooperative, aircraft evasion strategies from a missile that is using such guidance laws were also derived.

For adversaries with first-order dynamics it was shown that, depending on the initial conditions, and in contrast to the optimal one-on-one evasion strategy, the optimal cooperative target maneuver is either constant or arbitrary. These types of maneuvers are also the optimal ones for the defender missile.

A prerequisite to applying the optimal target and defender cooperative strategies, or the optimal one-on-one target evasive maneuver, is knowing the guidance strategy used by the attacking missile. This knowledge may be available a priori or acquired during the early stages of the engagement by an online identification scheme.

It was shown that cooperation allows the defender to intercept the attacking missile with a zero miss distance even in a scenario in which it has an order of magnitude maneuverability disadvantage. In such a scenario the target aircraft acts like a bait and lures in the attacking missile. In cooperating and helping its defender missile the target pays a penalty in the form of a slightly enlarged miss distance between it and the missile.

The hit-to-kill performance that is achievable, due to cooperation, even when using a very limited defending missile, facilitates the future use of relatively small defending missiles to protect aircraft from homing missiles.

Appendix A: One-On-One Optimal Evasion: Special Cases

In this Appendix we provide the specific optimal evasion strategies against the linear guidance strategies discussed in Sec. III: namely, PN, APN, and OGL.

I. Evasion from PN-Guided Missiles

If the missile uses PN guidance of Eqs. (15) and (18) with a constant N'_{PN}, then the gains in Eq. (26) become

$$K_1 = \frac{N'_{\mathrm{PN}}}{t^2_{\mathrm{go}_{MT}}}; \qquad K_2 = \frac{N'_{\mathrm{PN}}}{t_{\mathrm{go}_{MT}}}; \qquad \mathbf{K}_M = [0]$$
$$\mathbf{K}_T = [0]; \qquad K_{u_T} = 0 \tag{A1}$$

As in this case

$$K_2 = K_1 t_{\mathrm{go}_{MT}} \tag{A2}$$

we obtain from Eqs. (48) that

$$\phi_{12} = \phi_{11} t_{\mathrm{go}_{MT}} \tag{A3}$$

To compute the optimal target evasion strategy of Eq. (46) we need to solve the remaining terms in Eqs. (48) that satisfy

$$\begin{cases} \frac{\mathrm{d}\phi_{11}}{\mathrm{d}t_{\mathrm{go}_{MT}}} = -d_M N'_{\mathrm{PN}} \phi_{11}/t_{\mathrm{go}_{MT}} + \boldsymbol{\phi}_{1M} \mathbf{B}_M N'_{\mathrm{PN}}/t^2_{\mathrm{go}_{MT}}; & \phi_{11}(0) = 1 \\ \frac{\mathrm{d}\boldsymbol{\phi}_{1M}}{\mathrm{d}t_{\mathrm{go}_{MT}}} = -\mathbf{C}_M \phi_{11} t_{\mathrm{go}_{MT}} + \boldsymbol{\phi}_{1M} \mathbf{A}_M; & \boldsymbol{\phi}_{1M}(0) = [0] \\ \frac{\mathrm{d}\boldsymbol{\phi}_{1T}}{\mathrm{d}t_{\mathrm{go}_{MT}}} = \mathbf{C}_T \phi_{11} t_{\mathrm{go}_{MT}} + \boldsymbol{\phi}_{1T} \mathbf{A}_T; & \boldsymbol{\phi}_{1T}(0) = [0] \end{cases} \tag{A4}$$

Note that the first two equations above are independent from the third one. This set of equations can be solved numerically, as was shown in [10] using a simple Simulink block diagram. A closed-form analytical solution exists for the case in which it is assumed that the target has ideal dynamics (i.e., $\mathbf{A}_T = \mathbf{B}_T = \mathbf{C}_T = 0$, $d_T = 1$), the missile has first-order strictly proper dynamics (i.e., $\mathbf{A}_M = -1/\tau_M$, $\mathbf{B}_M = 1/\tau_M$, $\mathbf{C}_M = 1$, $d_M = 0$), and N'_{PN} is an integer. In such a case, as was shown in [7], Eqs. (A4) have the following closed-form solutions:

$$\phi_{12} = \begin{cases} \tau_M \exp(-\theta_{MT})[\theta_{MT} - \theta_{MT}^2/2] & N'_{\mathrm{PN}} = 3 \\ \tau_M \exp(-\theta_{MT})[\theta_{MT} - \theta_{MT}^2 + \theta_{MT}^3/6] & N'_{\mathrm{PN}} = 4 \\ \tau_M \exp(-\theta_{MT})[\theta_{MT} - 3\theta_{MT}^2/2 + \theta_{MT}^3/2 - \theta_{MT}^4/24] & N'_{\mathrm{PN}} = 5 \end{cases} \tag{A5}$$

$$\phi_{1M} = \begin{cases} \tau_M^2 \exp(-\theta_{MT})[-\theta_{MT}^2/2 + \theta_{MT}^3/6] & N'_{\mathrm{PN}} = 3 \\ \tau_M^2 \exp(-\theta_{MT})[-\theta_{MT}^2/2 + \theta_{MT}^3/3 - \theta_{MT}^4/24] & N'_{\mathrm{PN}} = 4 \\ \tau_M^2 \exp(-\theta_{MT})[-\theta_{MT}^2/2 + \theta_{MT}^3/2 - \theta_{MT}^4/8 + \theta_{MT}^5/120] & N'_{\mathrm{PN}} = 5 \end{cases} \tag{A6}$$

and $\phi_{1T} = 0$. The switching function of Eq. (38) in this case is

$$s_{MT} = \phi_{12} \tag{A7}$$

and the missile–target zero-effort miss (Z_{MT}) of Eq. (33) satisfies

$$Z_{MT} = \phi_{12}(\dot{y}_{MT} + y_{MT}/t_{\mathrm{go}_{MT}}) + \phi_{1M} a_M \tag{A8}$$

Assuming the target has first-order strictly proper dynamics instead of ideal (i.e., $\mathbf{A}_T = -1/\tau_T$, $\mathbf{B}_T = 1/\tau_T$, $\mathbf{C}_T = 1$, and $d_T = 0$) results in identical solutions for ϕ_{12} and ϕ_{1M}, as in Eqs. (A5) and (A6), respectively, whereas the solution for ϕ_{1T} is nonzero. The switching function for this case is

$$s_{MT} = \phi_{1T}/\tau_T \tag{A9}$$

and the zero-effort-miss distance is

$$Z_{MT} = \phi_{12}(\dot{y}_{MT} + y_{MT}/t_{\mathrm{go}_{MT}}) + \phi_{1M} a_M + \phi_{1T} a_T \tag{A10}$$

II. Evasion from APN-Guided Missiles

If the missile uses APN guidance of Eqs. (15) and (20), then the gains in Eq. (26) become

$$K_1 = \frac{N'_{\mathrm{APN}}}{t_{\mathrm{go}_{MT}}^2}; \qquad K_2 = \frac{N'_{\mathrm{APN}}}{t_{\mathrm{go}_{MT}}}; \qquad \mathbf{K}_M = [0]$$
$$\mathbf{K}_T = \frac{N'_{\mathrm{APN}}\mathbf{C}_T}{2}; \qquad K_{u_T} = \frac{N'_{\mathrm{APN}} d_T}{2} \tag{A11}$$

As for PN, Eq. (A2) and, consequently, Eq. (A3) are satisfied. For computing the switching surface of the optimal target evasion strategy of Eq. (46), the following set of equations from Eq. (48) needs to be solved:

$$\begin{cases} \frac{\mathrm{d}\phi_{11}}{\mathrm{d}t_{\mathrm{go}_{MT}}} = -d_M N'_{\mathrm{APN}}\phi_{11}/t_{\mathrm{go}_{MT}} + \boldsymbol{\phi}_{1M}\mathbf{B}_M N'_{\mathrm{APN}}/t_{\mathrm{go}_{MT}}^2; & \phi_{11}(0) = 1 \\ \frac{\mathrm{d}\boldsymbol{\phi}_{1M}}{\mathrm{d}t_{\mathrm{go}_{MT}}} = -\mathbf{C}_M\phi_{11}t_{\mathrm{go}_{MT}} + \boldsymbol{\phi}_{1M}\mathbf{A}_M; & \boldsymbol{\phi}_{1M}(0) = [0] \\ \frac{\mathrm{d}\boldsymbol{\phi}_{1T}}{\mathrm{d}t_{\mathrm{go}_{MT}}} = (1 - d_M N'_{\mathrm{APN}}/2)\mathbf{C}_T\phi_{11}t_{\mathrm{go}_{MT}} & \\ \quad + \boldsymbol{\phi}_{1M}\mathbf{B}_M\mathbf{C}_T N'_{\mathrm{APN}}/2 + \boldsymbol{\phi}_{1T}\mathbf{A}_T; & \boldsymbol{\phi}_{1T}(0) = [0] \end{cases} \tag{A12}$$

Note that the first two equations are identical to those of PN appearing in Eq. (A4), and here too they are independent from the third one. For the case in which it is assumed that the target has ideal dynamics (i.e., $\mathbf{A}_T = \mathbf{B}_T = \mathbf{C}_T = 0$, $d_T = 1$), the missile has first-order strictly proper dynamics (i.e., $\mathbf{A}_M = -1/\tau_M$, $\mathbf{B}_M = 1/\tau_M$, $\mathbf{C}_M = 1$, $d_M = 0$), and N'_{APN} is an integer, the solutions of ϕ_{12} and $\boldsymbol{\phi}_{1M}$ are identical to that of PN given in Eqs. (A5) and (A6), respectively. Also $\phi_{1T} = 0$.

The switching function of Eq. (38) in this case is

$$s_{MT} = \phi_{12} + \phi_{1M} N'_{\mathrm{APN}}/(2\tau_M) \tag{A13}$$

and Z_{MT} satisfies Eq. (A8).

Remark 7. Comparing Eq. (A13) to Eq. (A7) we note that the optimal evasion strategy of a target with ideal dynamics, from a missile with first-order strictly proper dynamics guided by APN, is different from that of evasion when PN is used for guidance. However, the expressions for the zero-effort miss of these two evasion problems are identical, as the solutions for ϕ_{12} and $\boldsymbol{\phi}_{1M}$ are identical.

Assuming the target has first-order strictly proper dynamics instead of ideal (i.e., $\mathbf{A}_T = -1/\tau_T$, $\mathbf{B}_T = 1/\tau_T$, $\mathbf{C}_T = 1$, and $d_T = 0$) does not affect the solutions for ϕ_{12} and ϕ_{1M}, whereas, as for PN, the solution for ϕ_{1T} is nonzero. The switching function for this case is now

$$s_{MT} = \phi_{1M} N'_{\mathrm{APN}}/(2\tau_M) + \phi_{1T}/\tau_T \tag{A14}$$

and the expression for the zero-effort miss is identical to that given in Eq. (A10).

III. Evasion from OGL-Guided Missiles

If the missile uses OGL of Eqs. (15), (21), and (22), then the gains in Eq. (26) become

$$K_1 = \frac{N'_{\mathrm{OGL}}}{t_{\mathrm{go}_{MT}}^2}; \qquad K_2 = \frac{N'_{\mathrm{OGL}}}{t_{\mathrm{go}_{MT}}}; \qquad \mathbf{K}_M = -\frac{N'_{\mathrm{OGL}}\psi(\theta_{MT})\mathbf{C}_M}{\theta_{MT}^2}$$
$$\mathbf{K}_T = \frac{N'_{\mathrm{OGL}}\mathbf{C}_T}{2}; \qquad K_{u_T} = \frac{N'_{\mathrm{OGL}} d_T}{2} \tag{A15}$$

with N'_{OGL} being time-varying [see Eq. (21)].

Once again Eqs. (A2) and (A3) are satisfied. And for computing the switching surface of the optimal target evasion strategy of Eq. (46), the following set of equations from Eq. (48) needs to be solved:

$$\begin{cases} \frac{\mathrm{d}\phi_{11}}{\mathrm{d}t_{\mathrm{go}_{MT}}} = -d_M N'_{\mathrm{OGL}}\phi_{11}/t_{\mathrm{go}_{MT}} + \boldsymbol{\phi}_{1M}\mathbf{B}_M N'_{\mathrm{OGL}}/t_{\mathrm{go}_{MT}}^2; & \phi_{11}(0) = 1 \\ \frac{\mathrm{d}\boldsymbol{\phi}_{1M}}{\mathrm{d}t_{\mathrm{go}_{MT}}} = (d_M f(\theta_{MT}) - 1)\mathbf{C}_M\phi_{11}t_{\mathrm{go}_{MT}} + \boldsymbol{\phi}_{1M}(\mathbf{A}_M - \mathbf{B}_M\mathbf{C}_M f(\theta_{MT})); & \boldsymbol{\phi}_{1M}(0) = [0] \\ \frac{\mathrm{d}\boldsymbol{\phi}_{1T}}{\mathrm{d}t_{\mathrm{go}_{MT}}} = (1 - d_M N'_{\mathrm{OGL}}/2)\mathbf{C}_T\phi_{11}t_{\mathrm{go}_{MT}} + \boldsymbol{\phi}_{1M}\mathbf{B}_M\mathbf{C}_T N'_{\mathrm{OGL}}/2 + \boldsymbol{\phi}_{1T}\mathbf{A}_T; & \boldsymbol{\phi}_{1T}(0) = [0] \end{cases} \tag{A16}$$

where

$$f(\theta_{MT}) = N'_{\mathrm{OGL}}(\theta_{MT})\psi(\theta_{MT})/\theta_{MT}^2 \tag{A17}$$

Once again the first two equations in Eqs. (A16) are independent from the third one. For the case in which it is assumed that the target has ideal dynamics (i.e., $\mathbf{A}_T = \mathbf{B}_T = \mathbf{C}_T = 0$ and $d_T = 1$), the solution of the third equation results with $\phi_{1T}=0$ and the switching function of Eq. (38) in this case is

$$s_{MT}=d_T(1-d_M N'_{\rm OGL}/2)\phi_{12}+\boldsymbol{\phi}_{1M}\mathbf{B}_M N'_{\rm OGL}/2 \tag{A18}$$

and Z_{MT} of Eq. (33) satisfies

$$Z_{MT}=\phi_{12}(\dot{y}_{MT}+y_{MT}/t_{{\rm go}_{MT}})+\boldsymbol{\phi}_{1M}\boldsymbol{x}_M \tag{A19}$$

Remark 8. If the missile has first-order strictly proper dynamics (i.e., $\mathbf{A}_M=-1/\tau_M$, $\mathbf{B}_M=1/\tau_M$, $\mathbf{C}_M=1$, $d_M=0$), then ϕ_{11}, ϕ_{12}, ϕ_{1M}, and ϕ_{1T} will be identically zero, resulting in a target–missile zero-effort miss distance that is identical to zero, no matter the evasion strategy of the target and the initial conditions. This is because OGL was designed taking into account such missile dynamics and assuming unbounded control.

Appendix B: Cooperative Pursuit and Evasion: Special Cases

In this Appendix we provide the specific optimal cooperative evasion and pursuit strategies, for the target and its defender, for the cases in which the missile uses the linear guidance strategies discussed in Sec. III: namely, PN, APN, and OGL.

I. Missile Uses PN

If the missile uses PN guidance, with the gains given in Eq. (A1), then the differential equations for ϕ_{52}, $\boldsymbol{\phi}_{5M}$, and $\boldsymbol{\phi}_{5T}$ from Eq. (85) are

$$\begin{cases}\frac{{\rm d}\phi_{52}}{{\rm d}t_{\rm go}}=(1-d_M N'_{\rm PN})\phi_{52}/(t_{\rm go}+\Delta t)+N'_{\rm PN}\boldsymbol{\phi}_{5M}\mathbf{B}_M/(t_{\rm go}+\Delta t); & \phi_{52}(0)=0\\ \frac{{\rm d}\boldsymbol{\phi}_{5M}}{{\rm d}t_{\rm go}}=-\mathbf{C}_M\phi_{52}+\boldsymbol{\phi}_{5M}\mathbf{A}_M+t_{\rm go}\mathbf{C}_M; & \boldsymbol{\phi}_{5M}(0)=[0]\\ \frac{{\rm d}\boldsymbol{\phi}_{5T}}{{\rm d}t_{\rm go}}=\mathbf{C}_T\phi_{52}+\boldsymbol{\phi}_{5T}\mathbf{A}_T; & \boldsymbol{\phi}_{5T}(0)=[0]\end{cases} \tag{B1}$$

Assuming first-order strictly proper acceleration dynamics for the missile and the target, Eq. (B1) degenerates to the following three scalar equations:

$$\begin{cases}\frac{{\rm d}\phi_{52}}{{\rm d}t_{\rm go}}=\phi_{52}/(t_{\rm go}+\Delta t)+N'_{\rm PN}\phi_{5M}/(\tau_M(t_{\rm go}+\Delta t)); & \phi_{52}(0)\\ \frac{{\rm d}\phi_{5M}}{{\rm d}t_{\rm go}}=-\phi_{52}-\phi_{5M}/\tau_M+t_{\rm go}; & \phi_{5M}(0)\\ \frac{{\rm d}\phi_{5T}}{{\rm d}t_{\rm go}}=\phi_{52}-\phi_{5T}/\tau_T; & \phi_{5T}(0)\end{cases} \tag{B2}$$

The target's switching surface in this case is

$$s_{MD_1}=\phi_{5T}/\tau_T \tag{B3}$$

II. Missile Uses APN

If the missile uses APN guidance, with the gains given in Eq. (A11), then the differential equations for ϕ_{52} and $\boldsymbol{\phi}_{5M}$ are identical to those given in Eq. (B1), with $N'_{\rm APN}$ replacing $N'_{\rm PN}$. For $\boldsymbol{\phi}_{5T}$ the differential equation is

$$\frac{{\rm d}\boldsymbol{\phi}_{5T}}{{\rm d}t_{\rm go}}=(1-d_M N'_{\rm APN}/2)\phi_{52}\mathbf{C}_T+\boldsymbol{\phi}_{5M}\mathbf{B}_M\mathbf{C}_T N'_{\rm APN}/2+\boldsymbol{\phi}_{5T}\mathbf{A}_T \tag{B4}$$

Assuming first-order strictly proper acceleration dynamics for the missile and the target we obtain for ϕ_{52} and $\boldsymbol{\phi}_{5M}$ the same differential equations as for PN in Eq. (B2). For ϕ_{5T} we obtain the following scalar differential equation:

$$\frac{{\rm d}\phi_{5T}}{{\rm d}t_{\rm go}}=\phi_{52}+N'_{\rm APN}\phi_{5M}/(2\tau_M)-\phi_{5T}/\tau_T \tag{B5}$$

The target's switching surface has the same form as that of PN, given in Eq. (B3), but the value of ϕ_{5T} is different.

III. Missile Uses OGL

If the missile uses OGL, with the gains given in Eq. (A15), then the differential equations for ϕ_{52}, $\boldsymbol{\phi}_{5M}$, and $\boldsymbol{\phi}_{5T}$ from Eq. (85) are

$$\begin{cases}\frac{{\rm d}\phi_{52}}{{\rm d}t_{\rm go}}=(1-d_M N'_{\rm OGL})\phi_{52}/(t_{\rm go}+\Delta t)+N'_{\rm OGL}\boldsymbol{\phi}_{5M}\mathbf{B}_M/(t_{\rm go}+\Delta t); & \phi_{52}(0)=0\\ \frac{{\rm d}\boldsymbol{\phi}_{5M}}{{\rm d}t_{\rm go}}=[d_M f(\theta_{MT})-1]\mathbf{C}_M\phi_{52}+\boldsymbol{\phi}_{5M}[\mathbf{A}_M-f(\theta_{MT})\mathbf{B}_M\mathbf{C}_M]+t_{\rm go}\mathbf{C}_M; & \boldsymbol{\phi}_{5M}(0)=[0]\\ \frac{{\rm d}\boldsymbol{\phi}_{5T}}{{\rm d}t_{\rm go}}=(1-d_M N'_{\rm OGL}/2)\mathbf{C}_T\phi_{52}+\boldsymbol{\phi}_{5M}\mathbf{B}_M\mathbf{C}_T N'_{\rm OGL}/2+\boldsymbol{\phi}_{5T}\mathbf{A}_T; & \boldsymbol{\phi}_{5T}(0)=[0]\end{cases} \tag{B6}$$

where $N'_{\rm OGL}$ is time-varying and $f(\theta_{MT})$ is given in Eq. (A17).

Assuming first-order strictly proper acceleration dynamics for the missile and the target, Eq. (B6) degenerates to the following three scalar equations:

$$\begin{cases}\frac{{\rm d}\phi_{52}}{{\rm d}t_{\rm go}}=\phi_{52}/(t_{\rm go}+\Delta t)+N'_{\rm OGL}\phi_{5M}/(\tau_M(t_{\rm go}+\Delta t)); & \phi_{52}(0)=0\\ \frac{{\rm d}\phi_{5M}}{{\rm d}t_{\rm go}}=-\phi_{52}-\phi_{5M}[1+f(\theta_{MT})]/\tau_M+t_{\rm go}; & \phi_{5M}(0)=0\\ \frac{{\rm d}\phi_{5T}}{{\rm d}t_{\rm go}}=\phi_{52}+\phi_{5M}N'_{\rm OGL}/2-\phi_{5T}/\tau_T; & \phi_{5T}(0)=0\end{cases} \tag{B7}$$

Note that here, in contrast to the one-on-one evasion problem from an OGL missile (presented in Appendix A) the transition matrix element ϕ_{51}, ϕ_{52}, ϕ_{5M}, and ϕ_{5T} (compared with ϕ_{11}, ϕ_{12}, ϕ_{1M}, and ϕ_{1T}) are nonzero.

The target's switching surface has the same form as that of PN, given in Eq. (B3), but the value of ϕ_{5T} is different.

Acknowledgment

This work was sponsored by the U.S. Air Force Office of Scientific Research, Air Force Material Command, under grant number FA8655-09-1-3051.

References

[1] Zarchan, P., *Tactical and Strategic Missile Guidance*, Progress in Astronautics and Aeronautics, Vol. 176, AIAA, Washington, D.C., 1997.

[2] Yuan, L. C., "Homing and Navigational Courses of Automatic Target-

Seeking Devices," *Journal of Applied Physics*, Vol. 19, No. 12, 1948, pp. 1122–1128.
doi:10.1063/1.1715028

[3] Garber, V., "Optimum Intercept Laws for Accelerating Targets," *AIAA Journal*, Vol. 6, No. 11, 1968, pp. 2196–2198.
doi:10.2514/3.4962

[4] Cottrell, G. R., "Optimal Intercept Guidance for Short-Range Tactical Missiles," *AIAA Journal*, Vol. 9, No. 7, 1971, pp. 1414–1415.
doi:10.2514/3.6369

[5] Asher, R., and Matuszewski, J., "Optimal Guidance with Maneuvering Targets," *Journal of Spacecraft and Rockets*, Vol. 11, No. 3, 1974, pp. 204–206.
doi:10.2514/3.62041

[6] Julich, P., and Borg, D., "Proportional Navigation vs an Optimally Evading, Constant-Speed Target in Two Dimensions," *Journal of Aircraft*, Vol. 7, No. 12, 1970, pp. 1454–1457.
doi:10.2514/3.30190.

[7] Shinar, J., and Steinberg, D., "Analysis of Optimal Evasive Maneuvers Based on a Linearized Two-Dimensional Kinematic Model," *Journal of Aircraft*, Vol. 14, No. 8, 1977, pp. 795–802.
doi:10.2514/3.58855

[8] Forte, I., Steinberg, A., and Shinar, J., "The Effects of Non-Linear Kinematics in Optimal Evasion," *Optimal Control Applications and Methods*, Vol. 4, 1983, pp. 139–152.
doi:10.1002/oca.4660040204

[9] Shinar, J., Rotsztein, Y., and Bezner, E., "Analysis of Three-Dimensional Optimal Evasion with Linearized Kinematics," *Journal of Guidance and Control*, Vol. 2, No. 5, 1979, pp. 353–360.
doi:10.2514/3.55889

[10] Gutman, S., *Applied Min-Max Approach to Missile Guidance and Control*, Progress in Astronautics and Aeronautics, Vol. 209, AIAA, Reston, VA, 2005, pp. 232–236.

[11] Gutman, S., and Ben-Aharon, O., "Proportional Navigation Miss Distance in the Presence of Bounded Inputs," *Journal of Guidance, Control, and Dynamics*, Vol. 32, No. 4, 2009, pp. 1143–1151.
doi:10.2514/1.41713

[12] Imado, F., and Miwa, S., "Fighter Evasive Boundaries Against Missiles," *Computers and Mathematics with Applications*, Vol. 18, No. 1, 1989, pp. 1–14.
doi:10.1016/0898-1221(89)90120-X

[13] Boyell, L. R., "Defending a Moving Target Against Missile or Torpedo Attack," *IEEE Transactions on Aerospace and Electronic Systems*, Vol. AES-12, No. 4, 1976, pp. 522–526.
doi:10.1109/TAES.1976.308338

[14] Shneydor, N. A., "Comments on "Defending a Moving Target Against Missile or Torpedo Attack," *IEEE Transactions on Aerospace and Electronic Systems*, Vol. 13, No. 3, 1977, pp. 321.
doi:10.1109/TAES.1977.308401

[15] Boyell, R. L., "Counterweapon Aiming for Defence of a Moving Target," *IEEE Transactions on Aerospace and Electronic Systems*, Vol. 16, No. 3, 1980, pp. 402–408.
doi:10.1109/TAES.1980.308911

[16] Rusnak, I., "The Lady, the Bandits and the Body-Guard Game," *The 44th Israel Annual Conference on Aerospace Science* [CD-ROM], Feb. 2004.

[17] Rusnak, I., "Acceleration Requirements in Defense Against Missile Attack," *The 47th Israel Annual Conference on Aerospace Science* [CD-ROM], Feb. 2007.

[18] Rusnak, I., "Guidance Laws in Defense Against Missile Attack," *IEEE 25th Convention of Electrical and Electronic Engineers in Israel*, Inst. of Electrical and Electronics Engineers, Piscataway, NJ, Dec. 2008.

[19] Perelman, A., Shima, T., and Rusnak, I., "Cooperative Differential Games Strategies for Active Aircraft Protection from a Homing Missile," AIAA Guidance, Navigation, and Control Conference, Toronto, AIAA Paper 2010-7878, 2010.

[20] Ratnoo, A., and Shima, T., "Line-of-Sight Interceptor Guidance for Defending an Aircraft," *Journal of Guidance, Control, and Dynamics*, Vol. 34, No. 2, 2011, pp. 522–532.
doi:10.2514/1.50572

[21] Shaferman, V., and Shima, T., "Cooperative Multiple Model Adaptive Guidance for an Aircraft Defending Missile," *Journal of Guidance, Control, and Dynamics*, Vol. 33, No. 6, 2010, pp. 1801–1813.
doi:10.2514/1.49515.

[22] Bryson, E. A., and Ho, C. Y., *Applied Optimal Control*, Blaisdell, Waltham, MA, 1969.